PHYSICS AND CHEMISTRY OF SOLID STATE
V. 26, No. 2 (2025) pp. 277-284

Section: Physics

DOI: 10.15330/pcss.26.2.277-284

Vasyl Stefanyk Precarpathian National University

ФІЗИКА І ХІМІЯ ТВЕРДОГО ТІЛА
Т. 26, № 2 (2025) С. 277-284

Фізико-математичні науки

PACS: 75.50.Gg

ISSN 1729-4428 (Print)
ISSN 2309-8589 (Online)

S.K. Sushant[1,3,4], Suresh Kuri[2], M.K. Rendale[3], S.N. Mathad[1]

Soft-Hard Ferrite Composites by Green Synthesis: Structural and Magnetic Properties

[1]*Department of Engineering Physics, K L E Institute of Technology, Hubballi, Karnataka, India,* sushantsk949@gmail.com [1,3,4], physicssiddu@gmail.com[1];
[2]*Department of Electronics and Communication Engineering, KLS Gogte Institute of Technology, Belagavi, Karnataka, India;*
[3]*Department of Physics, KLS Gogte Institute of Technology, Belagavi, Karnataka, India,* dr.mkrendale@git.edu;
[4]*Visvesvaraya Technological University, Belagavi, Karnataka, India*

This work reports the structural and magnetic properties studies of composites of $Mg_{0.42}Zn_{0.30}Co_{0.28}Fe_2O_4$ and $Ba_{(1-x)}Sr_xFe_{12}O_{19}$ ferrites. The evolution of phase formation for composite ferrites was analysed by X-ray diffraction method. All synthesized samples have coexistence of both spinel and hexagonal structures with crystallite size decreasing (63nm to 59nm). SEM analysis revealed grain morphology with grain size increasing (173nm to 268nm). EDX analysis confirmed the successful incorporation of Co and Sr into the composite ferrites. VSM analysis illustrated the presence of both soft-hard magnetic nature. The prepared composite samples showed significant changes in the structural and magnetic properties depending on the weight percentage of the constituent phases, thereby providing valuable insights into their potential technological applications.

Keywords: Spinal ferrite; Hexa ferrite; Composites; Structural properties; Magnetic properties.

Received 29 October2024; Accepted 26 May 2025.

Introductions

The remarkable research carried out related to magnetic, electrical and optical capabilities of nano ferrites shows multifunctional materials that are have wide range of technological applications. These ferrite materials which has higher surface area and quantum effects are because of their nanoscale in size, which has a big impact on physical properties [1]. The composites like spinals and hexagonal ferrites are two most well-known varieties of nano ferrites; which gives all information related to crystal structural and magnetic properties and ultimately this can be used in different applications.

The spinal ferrites typical formula is AB_2O_4, trivalent ions like Fe^{3+} occupying the B-site and divalent metal ions occupying the A- Site. Spinal ferrites have cubic crystal structure and these ferrites are well-known for having low coercivity and high saturation magnetizations, two soft magnetic characteristics [2,3]. These properties help in the inductors, transformers and magnetic cores which demands effective transmissions benefits, which greatly for the usage of ferrites. conversely, ferrites with hexagonal crystal structure, such barium and strontium ferrites, which are categorized as hard ferrites due to their intricate structure. The hard ferrites are perfect for electromagnetic wave absorption, microwave devices and permanent magnets due to their high coercivity [4].

The composites called the combinations of Cobalt (Co) doped ferrites and Strontium (Sr) doped ferrites has shown in the recent year as a way to improve the magnetic characteristics of both the materials. The materials like cobalt ferrite are widely recognized for its high chemical stability, modest saturation magnetizations and strong coercivity because of these important characteristics, it may be used in many applications like biological aspects which includes magnetic hyperthermia and medical administration, as well as high-density magnetic storage and magnetic sensors [5]. Cobalt ferrite may be used for certain technical requirements by doping it with other ferrites, which enhances its magnetic and structural characteristics. Similarly, Sr-doped hexaferrites show improved thermal stability and magnetic anisotropy over undoped counterparts, which makes them perfect for high frequency applications. Both doped and undoped forms of these ferrites are frequently synthesized using a modified sol-gel auto-combustions process (MSG). The synthesis process helps us in producing nanocrystalline ferrites, because it has a various benefit, such as uniformity in composition, particle size and low temperature while synthesis. This synthesis processes work well particularly for creating materials with high homogeneity with purity, which is essential for maximum structural and magnetic properties [6-11].

The development of contemporary technology can be seen in the synthesizing and characterizing of these ferrite composites. These materials are used efficiently in different fields and in a variety of applications, such as biological imaging, environmental cleanup, and magnetic storage. To maximize their characteristics, they need to modified according to the different composition or method of preparation. This manuscript focuses on preparation of composites of soft and hard ferrites considering their weight ratios. Detailed structural and magnetic properties of the prepared samples have been reported. The synthesis technic employed in this case give high purity and uniform composition, leading to enhanced magnetic and structural characteristic properties.

I. Experimental procedure

1.1. Synthesis Process

The Cobalt doped Magnesium-Zinc and Strontium doped Barium Ferrite were prepared by using modified sol-gel auto combustion technique, all Metal nitrates (Mg $(NO_3)_2$, Co $(NO_3)_2$, Zn $(NO_3)_2$, Fe $(NO_3)_3$, Ba $(NO_3)_2$, and Sr $(NO_3)_2$) taken are dissolved in freshly prepared lemon juice which is rich in citric acid then heated till all liquid evaporated. As an end result we found that due to natural citric acid in lemon juice which acting as chelating agent in this reaction helps to get combusted and the fine powder needs to heated (950°C) to remove unwanted materials then all samples taking 50:50 composition of spinel ferrite samples from Co doped Mg-Zn ferrite and Hexa ferrite samples from Sr doped Br ferrite mixed in agate mortar grinded and heated in muffle furnace at 500°C as showed in flow chart [12,13].

$$Mg_{0.42}Zn_{0.3}Co_{0.28}Fe_2O_4 + Ba_{(1-x)}Sr_xFe_{12}O_{19}(x = 0,0.2,0.4,0.60.8,1.00) \xrightarrow{500^0C} \underbrace{Mg_{0.42}Zn_{0.3}Co_{0.28}Fe_2O_4 + Ba_{(1-x)}Sr_xFe_{12}O_{19}}_{\text{Composite ferrites}}$$

II. Characterization techniques

2.1. X-Ray Diffraction (XRD)

The spinel ferrite with x = 0.28 was mixed with hexaferrite (x = 0 to 1.0) to obtain CM00, CM02, CM04, CM06, CM08 and CM10 composite samples. These materials were verified by XRD analysis, as depicted in Fig. 2. The diffraction pattern confirmed the formation of

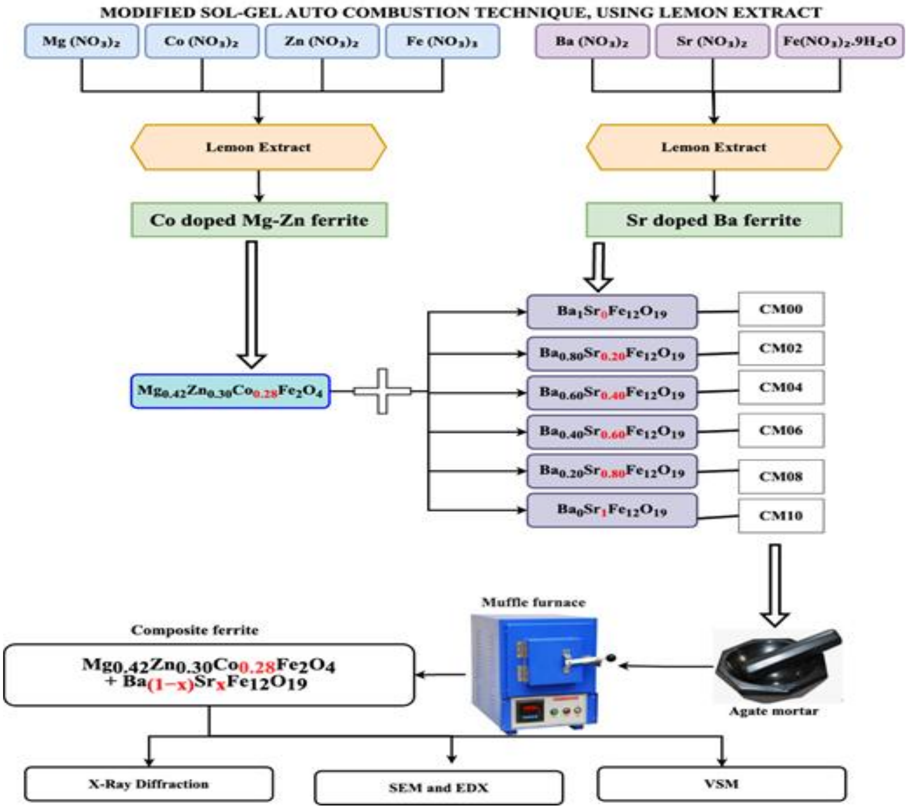

Fig. 1. Flow chart for Mg-Zn-Co soft ferrite and Ba-Sr hard ferrite composite nanoparticles.

a biphasic structure, containing both cubic spinel and hexagonal phases. The primary diffraction peaks corresponding to the cubic spinel structure of Co-doped Mg-Zn ferrite were observed at the prominent (311) plane, followed by other peaks at (111), (220), (400), (422), (511), (440), and (533). The hexaferrite phase was identified by the most prominent (110) peak, followed by peaks at (102), (107), (114), (203), and (217). The presence of these distinct peaks verifies the biphasic nature of the composite without the formation of secondary phases. However, some peaks were absent or merged due to structural distortions induced by Sr doping, crystallite size variations, and strain effects [14-16].

The crystallite size (D) was calculated using the Scherrer formula and is tabulated in Table 1. The crystallite size non-linearly decreased (from 63 nm to 59nm) with increasing Sr^{2+} doping in the composite samples. Initially, from CM00 to CM06, the crystallite size increased with Sr doping. This is because the smaller Sr^{2+} ion (1.26Å) attempted to occupy the Ba^{2+} (1.42 Å) site, leading to improved atomic packing and an increase in crystallite size. However, at higher Sr concentrations (CM08), the crystallite size decreased to 30 nm. This reduction is attributed to the increased internal strain caused by the smaller Sr^{2+} ions, which disrupts the crystal structure and limits crystallite growth. For the CM10 sample, Sr^{2+} ions were uniformly incorporated into the $Ba_0Sr_1Fe_{12}O_{19}$ structure, reducing internal strain and leading to an increase in crystallite size to 59 nm [17,18]. This indicates that in the composite samples, Sr doping primarily affects the hexagonal structure, while the spinel structure remains unchanged due to the constant Co content. Consequently, Sr substitution influences the interaction between the two phases, affecting both their crystallite size and magnetic properties [5,19].

2.2. Scanning Electron Microscopy (SEM) and EDX Characterization

The SEM micrographs of the composites (CM00 to CM10) are depicted in Fig. 3. They reveal that all composites prepared using MSG exhibit observable changes with increasing Sr ion doping. The SEM images contain both irregular and spherical-shaped grains present between flake-like grain structures.

As the Sr content increases, the grain size varies from 173 nm to 268nm for CM00 to CM10 samples, as shown

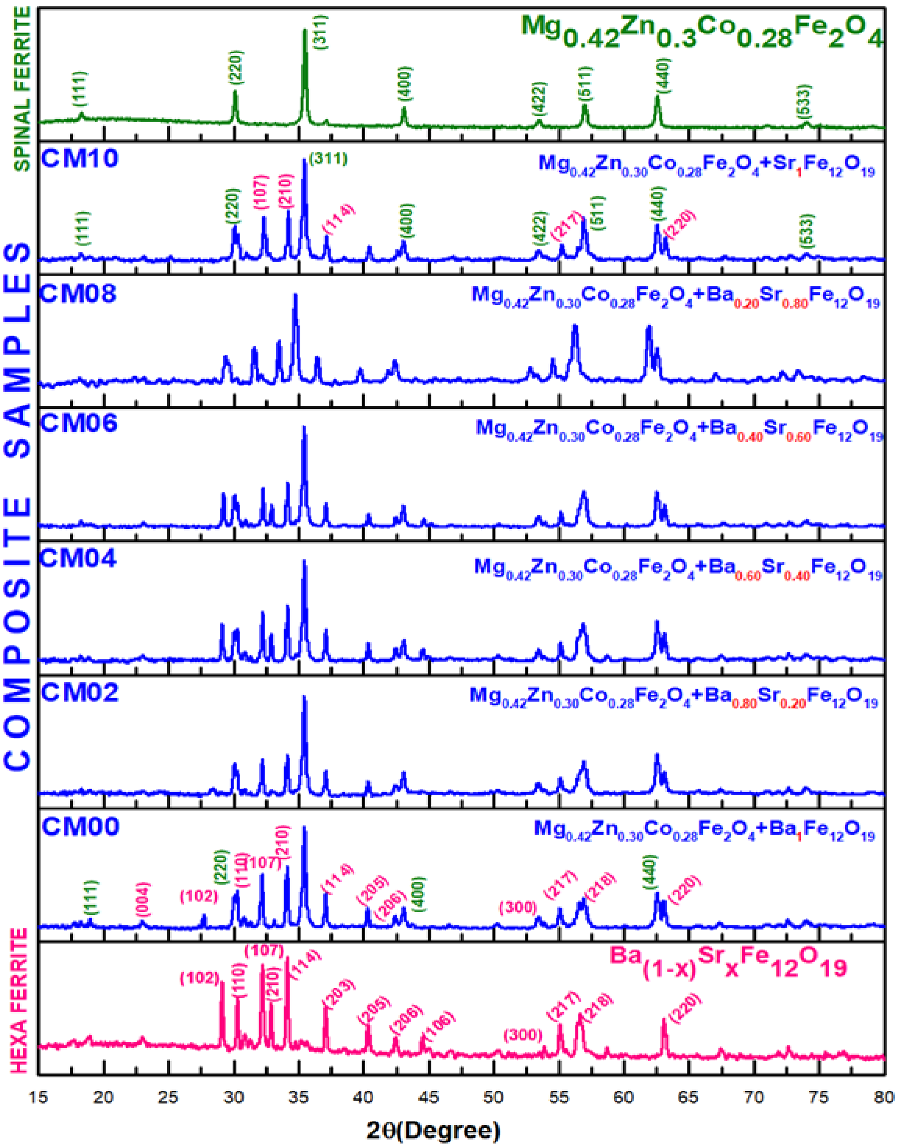

Fig. 2. X-ray Diffraction patterns of Mg-Zn-Co soft ferrite and Ba-Sr hard ferrite composite nanoparticles.

in Table 2. With the increase in Sr content, the flake-like structures begin to break, leading to grain fragmentation and increased porosity. This, in turn, affects the magnetic properties by increasing saturation magnetization [20-25].

Energy-dispersive X-ray (EDX) analysis confirms that Sr content increases while Ba content decreases, with Co and Zn content remaining constant. These elemental changes align with the expected stoichiometry of the prepared samples. Table 3 reveals that as Sr content increases, Ba is replaced. Specifically, the CM00 sample is prepared without Sr, while in CM10, Ba is absent, with Sr doping dominating. Overall, Fe content is the highest across all prepared samples, as shown in Fig. 4, suggesting that the ferrite phase structure has been successfully retained. Additionally, Co and Zn content remain nearly constant, while Sr content increases, as observed in Table 4. This indicates that the elemental distribution has a significant impact on phase stability and changes in grain

Table 1.

Crystallite size (D) for prepared composite samples.

Samples	Composite samples	Crystallite size D nm
CM00	$Mg_{0.42}Zn_{0.30}Co_{0.28}Fe_2O_4$+ $Ba_1Fe_{12}O_{19}$	63
CM02	$Mg_{0.42}Zn_{0.30}Co_{0.28}Fe_2O_4$+ $Ba_{0.8}Sr_{0.2}Fe_{12}O_{19}$	64
CM04	$Mg_{0.42}Zn_{0.30}Co_{0.28}Fe_2O_4$+ $Ba_{0.6}Sr_{0.4}Fe_{12}O_{19}$	65
CM06	$Mg_{0.42}Zn_{0.30}Co_{0.28}Fe_2O_4$+ $Ba_{0.4}Sr_{0.6}Fe_{12}O_{19}$	64
CM08	$Mg_{0.42}Zn_{0.30}Co_{0.28}Fe_2O_4$+ $Ba_{0.2}Sr_{0.8}Fe_{12}O_{19}$	30
CM10	$Mg_{0.42}Zn_{0.30}Co_{0.28}Fe_2O_4$+ $Sr_1Fe_{12}O_{19}$	59

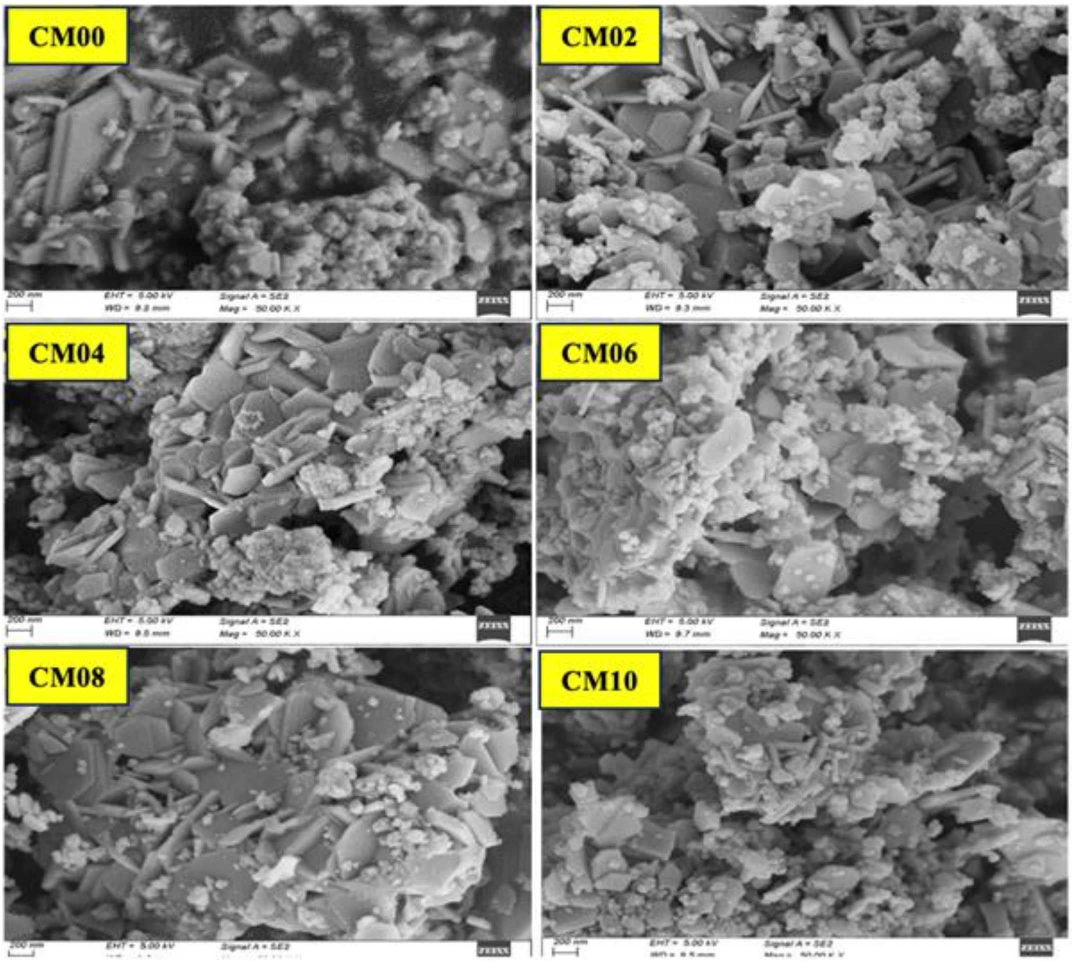

Fig. 3. SEM images of Mg-Zn-Co soft ferrite and Ba-Sr hard ferrite composite nanoparticles.

Table 2.

Average grain size of CM nanoferrites series.

Average Grain size of CM Series in nm					
CM00	**CM02**	**CM04**	**CM06**	**CM08**	**CM10**
173	223	237	255	263	268

Table 3.

Energy dispersive X-ray spectroscopy (EDX) analysis of all CM samples.

Samples	Elements	Mg	Fe	Co	Zn	Sr	Ba
CM00	Weight%	3.39	73.70	4.84	4.75	0.00	13.33
	Atomic%	8.14	77.14	4.80	4.75	0.00	5.67
CM02	Weight%	3.08	68.76	5.07	5.21	2.24	15.64
	Atomic%	7.61	74.04	5.17	4.79	1.54	6.85
CM04	Weight%	2.18	72.36	2.90	2.93	5.37	14.25
	Atomic%	5.45	78.80	2.99	2.73	3.73	6.31
CM06	Weight%	2.99	77.86	3.57	3.40	5.26	6.92
	Atomic%	7.08	80.11	3.48	2.99	3.45	2.89
CM08	Weight%	3.48	72.02	4.41	4.36	11.93	3.79
	Atomic%	8.24	74.20	4.31	3.83	7.84	1.59
CM10	Weight%	0.19	88.79	3.71	5.15	2.16	0.00
	Atomic%	0.44	90.13	3.57	4.46	1.40	0.00

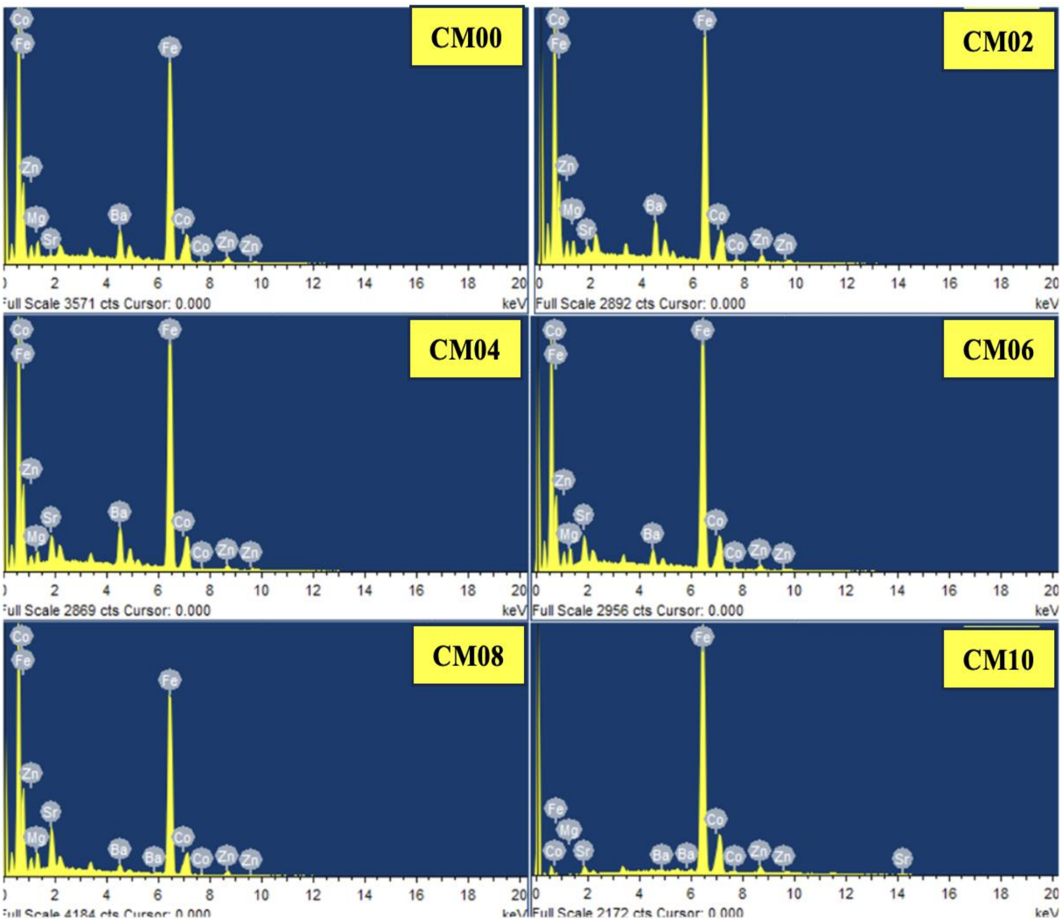

Fig. 4. EDX analysis of Mg-Zn-Co soft ferrite and Ba-Sr hard ferrite composite nanoparticles.

morphology [26-30].

Vibrating Sample Magnetometry (VSM)

The VSM analysis of all composite samples studied for magnetic characteristics study shows that the prepared composites affect the materials, which affects saturation magnetization (Ms), coercivity (Hc), and remanent magnetization (Mr) from Fig. 5 and related data from Table 4. The initial composition CM00, which has the lowest saturation magnetization values at 12.55 emu/g, indicates a comparatively weak magnetic reaction, and the last composite CM10, which has the highest values at 28.28 emu/g, shows the most significant magnetic response compared to other samples. This kind of change is preferred to be used in transformers, indicators, and other applications, which are effective in maintaining magnetic flux control to get Ms changes, suggests that the magnetic strength of the materials is efficiently adapted to different compositions or different synthesis circumstances, like selecting lemon as a fuel or sintering temperature. Considering coercivity with respect to CM04 with higher values at 526.53 Oe, which indicates elevated demagnetization, this elevated resistance to demagnetization. The lowest coercivity is at 409.82 Oe for CM01; on the other hand, it makes it extra terrific for

Table 4.

The saturation magnetization (Ms), coercivity (Hc), remanent magnetization (Mr) for all Composites samples.

Measurements	CM00	CM02	CM04	CM06	CM08	CM10
Magnetization (Ms) in emu/g	12.55	20.57	21.34	25.02	25.85	28.28
Coercivity (Hc) in emu/g	409.82	426.88	526.53	487.30	509.57	465.02
Retentivity (Mr) in emu/g	5.98	6.43	6.83	6.93	8.47	9.52

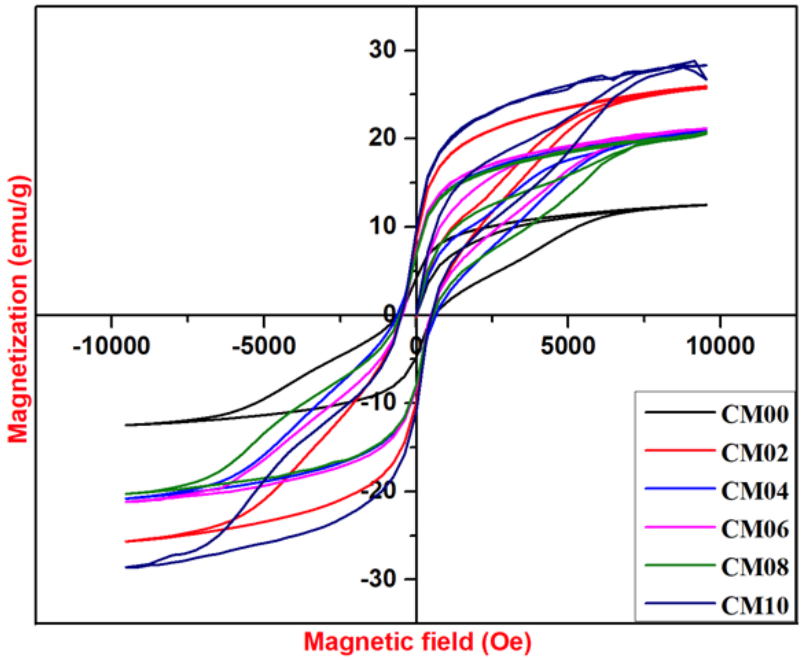

Fig 5. VSM analysis of Mg-Zn-Co soft ferrite and Ba-Sr hard ferrite composite nanoparticles.

smooth magnetic functions, where simple magnetization and demagnetization are beneficial. The prepared composites maintain the remanent magnetization values,, with the highest for CM10 at 9.52 emu/g, which is good for permanent magnets, and the lowest Mr recorded at 5.98 emu/g for CM00, with the worsen retention qualities, so it is potentially advisable to use in the permanent magnetic application [31-33].

The prepared samples revealed the exitance both soft-hard magnetic nature for spinel and hexaferrite phases, which are illustrated by these differences in magnetic properties across the prepared composite samples. The magnetization and anisotropy result from the direct impact of substitution such as cobalt and strontium on the exchange interactions. These prepared samples are used in applications like microwave absorption results technologies have a high saturation magnetization and controlled coercivity are crucial for performance optimizations. For example, CM10 shows Ms, moderate coercivity, and strong remanent magnetization are highly applicable for the feature scope. The overall outcomes show that it is crucial to modify the composition in order to control the magnetic study for specific technological uses [29,30].

Conclusion

This study concludes by providing information on the composite ferrites prepared and subjected to X-ray diffraction (XRD) analysis, successfully validating the synthesis of spinel ferrite and hexaferrite (biphasic) composite materials. A decrease in crystallite size (63nm to 59nm) was observed. SEM images revealed irregularly shaped grains embedded within a flake-like grain structure. As Sr content increased, the grain size also grew from 173 nm to 268 nm in the prepared samples. EDX analysis confirmed the elemental composition, showing that the Co and Zn content remained nearly constant, while Sr content increased by replacing Ba content. The VSM study revealed that composite ferrites improve magnetic properties, including an increase in Ms (12.55 emu/g to 28.28emu/g), moderate fluctuations in Hc (409 Oe to 465Oe) and strong Mr (5.98 emu/g to 9.52 emu/g) values (from CM00 to CM10), making them ideal due to the presence of both soft and hard ferrite phases. These unique properties make the materials attractive for applications in microwave absorber, magnetic recorder, and various other technological domains, where magnetic properties play a significant role.

Sushant S. K. – Assistant Professor, Ph.D.
Kuri Suresh – Associate Professor, Ph.D.
Rendale M. K. – Professor, Ph.D.
Mathad S. N. – . Associate Professor,Ph.D.

[1] Y. Mouhib, M. Belaiche, M. Elansary, C.A. Ferdi, and I. Guetni, *Multifunctional ferrite nanoparticles prepared from non-standard precursors: Structural, morphological, and magnetic study*, J Mol Struct, 1292, 136094 (2023); https://doi.org/10.1016/J.MOLSTRUC.2023.136094.

[2] T. Dippong, E. A. Levei, and O. Cadar, *Recent Advances in Synthesis and Applications of MFe_2O_4 (M = Co, Cu, Mn, Ni, Zn) Nanoparticles*, Nanomaterials, 11(6), 1560 (2021); https://doi.org/10.3390/NANO11061560.

[3] S.J. Salih and W.M. Mahmood, *Review on magnetic spinel ferrite (MFe_2O_4) nanoparticles: From synthesis to application*, Heliyon, 9(6), e16601 (2023); https://doi.org/10.1016/J.HELIYON.2023.E16601.

[4] U. Habiba, H. Rouf, S. H.-E. J. of Materials, and undefined 2017, *Structural and Magnetic Characterizations of Barium-Strontium-Ferrites using Hematite of Analytical Grade and Magnetite from Cox's Bazar Beach Sand Mineral*, academia.eduU Habiba, HK Rouf, SM HoqueEuropean Journal of Materials Science and Engineering, 2017•academia.edu, Accessed: Oct. 19, 2024.

[5] S. Kakati, M. K. Rendale, and S. N. Mathad, *Synthesis, Characterization, and Applications of $CoFe_2O_4$ and M-$CoFe_2O_4$ (M = Ni, Zn, Mg, Cd, Cu, RE) Ferrites: A Review*, International Journal of Self-Propagating High-Temperature Synthesis, 30(4), 189 (2021); https://doi.org/10.3103/S1061386221040038.

[6] M.K. Rendale, S.N. Mathad, and V. Puri, *Structural, mechanical and elastic properties of $Ni_{0.7-x}Co_xZn_{0.3}Fe_2O_4$ nano-ferrite thick films*, Microelectronics International, 34(2), 57 (2017); https://doi.org/10.1108/MI-02-2016-0009/FULL/XML.

[7] S.U. Durgadsimi, V.R. Kattimani, N.S. Maruti, A.B. Kulkarni, and S. N. Mathad, *Synthesis and structural analysis of nickel ferrite synthesized by co-precipitation method,* Eurasian Physical Technical Journal, 18(4), 14, (2021); https://doi.org/10.31489/2021NO4/14-19.

[8] I. Sabir, H. Mingxia, H. Anwar, M. Kashif, and Z. Yizhu, *Utilization of copper-doped zinc spinel ferrites nano-composites as battery-grade electrode materials for supercapattery device applications*, J Energy Storage, 112, 115498 (2025), https://doi.org/10.1016/J.EST.2025.115498.

[9] K. Tanbir, M. P. Ghosh, R. K. Singh, and S. Mukherjee, *Gd-doped soft Mn–Zn nanoferrites: synthesis, microstructural, magnetic and dielectric characterizations*, Journal of Materials Science: Materials in Electronics, 31 (4), 3529 (2020); https://doi.org/10.1007/S10854-020-02901-1.

[10] J. Mazurenko et al., *Analysis of the Structural, Morphological, and Elastic Properties of Nanosized $CuFe_2O_4$ Spinel Synthesized via Sol-Gel Self-Combustion Method*, Physics and Chemistry of Solid State, 25(2), 380 (2024); https://doi.org/10.15330/PCSS.25.2.380-390.

[11] V. S. Precarpathian, E. Turgut, E. Şenarslan, G. Merhan Muğlu, and S. Sarıtaş, *Assessment of titanium - tungsten iron oxide and their gas sensor application*, Physics and Chemistry of Solid State, 25(3), 498 (2024); https://doi.org/10.15330/PCSS.25.3.498-505.

[12] S.S. Kakati, T.M. Makandar, M.K. Rendale, and S.N. Mathad, *Green Synthesis Approach for Nanosized Cobalt Doped Mg–Zn through Citrus Lemon Mediated Sol–Gel Auto Combustion Method*, International Journal of Self-Propagating High-Temperature Synthesis, 31 (3), 131 (2022); https://doi.org/10.3103/S1061386222030049/TABLES/2.

[13] K.L. Routray, S. Saha, and D. Behera, *Green synthesis approach for nano sized $CoFe_2O_4$ through aloe vera mediated sol–gel auto combustion method for high frequency devices*, Mater. Chem. Phys., 224, 29 (2019); https://doi.org/10.1016/j.matchemphys.2018.11.073.

[14] M. R. Islam et al., *Structural, thermodynamic, and magnetic properties of $SrFe_{12}O_{19}$ hexaferrite modified by co-substitution of Cu and Gd*, RSC Adv, 14 (11), 7314 (2024); https://doi.org/10.1039/D3RA08878B.

[15] M. Sajjad et al., *Detailed analysis of structural and optical properties of spinel cobalt doped magnesium zinc ferrites under different substitutions*, Journal of Materials Science: Materials in Electronics, 31(23), 21779 (2020); https://doi.org/10.1007/S10854-020-04690-Z/FIGURES/13.

[16] P. Dhiman, G. Rana, A. Kumar, and G. Sharma, *Co Doped Mg–Zn Spinel Nano-ferrites as a Sustainable Magnetic Nano-photo-catalyst with Reduced Recombination for Photo Degradation of Crystal Violet*, J Inorg Organomet Polym Mater, 33(9), 2776 (2023); https://doi.org/10.1007/S10904-023-02698-6/FIGURES/12.

[17] A. Kumar, V. Agarwala, and D. Singh, *Effect of particle size of BaFe12O19 on the microwave absorption CHARACTERISTICS in X-band*, Progress In Electromagnetics Research M, 29, 223 (2013); https://doi.org/10.2528/PIERM13011604.

[18] M. R. Islam et al., *Structural, thermodynamic, and magnetic properties of SrFe12O19 hexaferrite modified by co-substitution of Cu and Gd*, RSC Adv, 14(11), 7314 (2024); https://doi.org/10.1039/D3RA08878B.

[19] S. U. Durgadsimi et al., *Synthesis, structural and electrical studies of Li-Ni-Zn ferrites synthesized by solid state reaction method*, Acta Periodica Technologica, 55, 47 (2024); https://doi.org/10.2298/APT2455047D.

[20] A. Elahi, M. Ahmad, I. Ali, and M. U. Rana, *Preparation and properties of sol–gel synthesized Mg-substituted Ni2Y hexagonal ferrites*, Ceram Int, 39(2), 983 (2013); https://doi.org/10.1016/J.CERAMINT.2012.07.016.

[21] M. Sundararajan et al., *A comparative study on $NiFe_2O_4$ and $ZnFe_2O_4$ spinel nanoparticles: Structural, surface chemistry, optical, morphology and magnetic studies*, Physica B Condens Matter, 644, 414232 (2022); https://doi.org/10.1016/J.PHYSB.2022.414232.

[22] T. R. Mehdiyev *et al.*, *Cluster aggregation OF $Ni_{1-x}Zn_xFe_2O_4$ ferrospinels*, J Magn Magn Mater, 587, 171326, (2023); https://doi.org/10.1016/J.JMMM.2023.171326.

[23] J. J. Kiptarus, K. K. Korir, D. N. Githinji, and H. K. Kiriamiti, *Improved photocatalytic performance of cobalt doped ZnS decorated with graphene nanostructures under ultraviolet and visible light for efficient hydrogen production*, Scientific Reports, 14(1), 1 (2024); https://doi.org/10.1038/s41598-024-72645-z.

[24] J. Hlosta et al., *Influence of calcination temperature and particle size distribution on the physical properties of $SrFe_{12}O_{19}$ and $BaFe_{12}O_{19}$ hexaferrite powder*s, Scientific Reports, 14(1), 1 (2024); https://doi.org/10.1038/s41598-024-67994-8.

[25] M.M. Arman, *Structural, morphological and magnetic properties of hexaferrite $BaCo_2Fe_{16}O_{27}$ nanoparticles and their efficient lead removal from water*, Appl Phys A Mater Sci Process, 128(12), 1 (2022); https://doi.org/10.1007/S00339-022-06244-Y/FIGURES/12.

[26] P. Kaur, A. Kaushik, and S. Singhal, *Comparative evaluation of photocatalytic performance of hexagonal ferrites procured via sol-gel route*, Mater Today Proc, 14, 426 (2019); https://doi.org/10.1016/J.MATPR.2019.04.165.

[27] M.A. Ahmed, E. García, L. Alonso, and J. M. Palacios, *A MS, SEM-EDX and XRD study of Ti or Cu-doped zinc ferrites as regenerable sorbents for hot coal gas desulfurization*, Appl Surf Sci, 156(1), 115 (2000); https://doi.org/10.1016/S0169-4332(99)00486-9.

[28] J.J. Kiptarus, K.K. Korir, D.N. Githinji, and H.K. Kiriamiti, *Improved photocatalytic performance of cobalt doped ZnS decorated with graphene nanostructures under ultraviolet and visible light for efficient hydrogen production*, Scientific Reports, 14(1), 1(2024); https://doi.org/10.1038/s41598-024-72645-z.

[29] M.M. Arman, *Structural, morphological and magnetic properties of hexaferrite $BaCo_2Fe_{16}O_{27}$ nanoparticles and their efficient lead removal from water*, Appl Phys A Mater Sci Process, 128(12), 1(2022); https://doi.org/10.1007/S00339-022-06244-Y/FIGURES/12.

[30] J. Hlosta et al., *Influence of calcination temperature and particle size distribution on the physical properties of $SrFe_{12}O_{19}$ and $BaFe_{12}O_{19}$ hexaferrite powders*, Scientific Reports, 14(1), 1 (2024); https://doi.org/10.1038/s41598-024-67994-8.

[31] M. Hussain et al., *Tuning the Magnetic Behavior of Zinc Ferrite via Cobalt Substitution: A Structural Analysis*, ACS Omega, 9(2), 2536 (2024); https://doi.org/10.1021/ACSOMEGA.3C07251.

[32] M. A. Rahman, M. T. Islam, M. S. J. Singh, M. Samsuzzaman, and M. E. H. Chowdhury, *Synthesis and characterization of Mg–Zn ferrite based flexible microwave composites and its application as SNG metamaterial*, Scientific Reports, 11(1), 1 (2021); https://doi.org/10.1038/s41598-021-87100-6.

[33] M. R. Patil, M. K. Rendale, S. N. Mathad, and R. B. Pujar, *Electrical and magnetic properties of Cd^{+2} doped Ni-Zn ferrites*, Inorganic and Nano-Metal Chemistry, 47(8), 1145 (2017); https://doi.org/10.1080/24701556.2017.1284097.

С. Какаті[1,3,4], Суреш Курі[2], М.К. Рендал[3], С.Н. Матхад[1]

Феритові композити легкої твердості, отримані методом зеленого синтезу: структурні та магнітні властивості

[1]*Кафедра інженерної фізики, Технологічний інститут KLE E, Хаббаллі, Карнатака, Індія, sushantsk949@gmail.com;*
[2]*Кафедра електроніки та комунікаційної інженерії, Технологічний інститут KLS Gogte, Белагаві, Карнатака, Індія;*
[3]*Кафедра фізики, Технологічний інститут KLS Gogte, Белагаві, Карнатака, Індія, dr.mkrendale@git.edu;*
[4]*Технологічний університет Вісвесварая, Белагаві, Карнатака, Індія, physicssiddu@gmail.com*

У роботі представлено дослідження структурних та магнітних властивостей композитів з феритів $Mg_{0.42}Zn_{0.30}Co_{0.28}Fe_2O_4$ та $Ba_{1-x}Sr_xFe_{12}O_{19}$. Еволюцію фазоутворення для композитних феритів проаналізовано методом Х-променевої дифракції. Усі синтезовані зразки містять співіснування як шпінельних, так і гексагональних структур зі зменшенням розміру кристалітів (від 63 нм до 59 нм). SEM-аналіз виявив морфологію зерен зі збільшенням розміру зерен (від 173 нм до 268 нм). EDX-аналіз підтвердив включення Co та Sr до композитних феритів. VSM-аналіз проілюстрував наявність як м'яких, так і твердих магнітних властивостей. Підготовлені композитні зразки показали значні зміни структурних та магнітних властивостей залежно від масового відсотка складових фаз, що дає цінну інформацію про їх потенційне технологічне застосування.

Ключові слова: Спінальний ферит; Гексаферит; Композити; Структурні властивості; Магнітні властивості.